Theor Appl Climatol (2010) 101:67–81
DOI 10.1007/s00704-009-0198-6

ORIGINAL PAPER

Global warming mitigation by sulphur loading in the stratosphere: dependence of required emissions on allowable residual warming rate

Alexey V. Eliseev · Alexandr V. Chernokulsky · Andrey A. Karpenko · Igor I. Mokhov

Received: 5 March 2009 / Accepted: 4 August 2009 / Published online: 4 September 2009

Abstract An approach to mitigate global warming via sulphur loading in the stratosphere (geoengineering) is studied, employing a large ensemble of numerical experiments with the climate model of intermediate complexity IAP RAS CM. The model is forced by the historical+SRES A1B anthropogenic greenhouse gases+tropospheric sulphates scenario for 1860–2100 with additional sulphur emissions in the stratosphere in the twenty-first century. Different ensemble members are constructed by varying values of the parameters governing mass, horizontal distribution and radiative forcing of the stratospheric sulphates. It is obtained that, given a global loading of the sulphates in the stratosphere, among those studied in this paper latitudinal distributions of geoengineering aerosols, the most efficient one at the global basis is that peaked between $50^\circ N$ and $70^\circ N$ and with a somewhat smaller burden in the tropics. Uniform latitudinal distribution of stratospheric sulphates is a little less efficient. Sulphur emissions in the stratosphere required to stop the global temperature at the level corresponding to the mean value for 2000–2010 amount to more than 10 TgS/year in the year 2100. These emissions may be reduced if some warming is allowed to occur in the twenty-first century. For instance, if the global temperature trend S_g in every decade of this century is limited not to exceed 0.10 K/decade (0.15 K/decade), geoengineering emissions of 4–14 TgS/year (2–7 TgS/year) would be sufficient. Even if the global warming is stopped, temperature changes in different regions still occur with a magnitude up to 1 K. Their horizontal pattern depends on implied latitudinal distribution of stratospheric sulphates. In addition, for the stabilised global mean surface air temperature, global precipitation decreases by about 10%. If geoengineering emissions are stopped after several decades of implementation, their climatic effect is removed within a few decades. In this period, surface air temperature may grow with a rate of several Kelvins per decade. The results obtained with the IAP RAS CM are further interpreted employing a globally averaged energy–balance climate model. With the latter model, an analytical estimate for sulphate aerosol emissions in the stratosphere required climate mitigation is obtained. It is shown that effective vertical localisation of the imposed radiative forcing is important for geoengineering efficiency.

A. V. Eliseev (✉) · A. V. Chernokulsky · A. A. Karpenko · I. I. Mokhov
A.M. Obukhov Institute of Atmospheric Physics RAS, 3 Pyzhevsky, 119017 Moscow, Russia
e-mail: eliseev@ifaran.ru, eliseev_av@mail.ru

1 Introduction

Global warming has been observed for the past few decades with a rate unprecedented for the period of instrumental meteorological observations (Trenberth et al. 2007). It is likely that a significant part of this warming is due to greenhouse anthropogenic influence on climate (Hegerl et al. 2007). Global surface air temperature T_g rise in the twenty-first century projected with state-of-the-art climate models under realistic scenarios of anthropogenic forcing attains 1.1–6.4 K depending on model and scenario (Meehl et al. 2007). If the real warming would be in the middle or, especially, in the upper part of this range, it would induce large and undesirable environmental changes.

As a result, it is tempting to develop a *geoengineering* strategy to mitigate the global warming without reducing emissions of greenhouse gases (Schneider 2001). One such approach concerns controlled emissions of sulphur species in the stratosphere to reduce the solar heating of the Earth and compensate for the warming radiative forcing of the long-lived greenhouse gases. Originally proposed by Budyko (1977) and based on observed climate cooling after volcanic eruptions, this approach gained a renewed interest recently (Schneider 1996, 2001; Izrael 2005; Crutzen 2006; Wigley 2006).

Volcanic eruptions serve as a natural, albeit incomplete, analogue for the proposed geoengineering scheme. As a result, response of climatic variables to past volcanism may be used to infer possible consequences and side effects of this approach. In particular, caution has been expressed due to widespread dryness developing after major volcanic eruptions (Groisman 1985; Trenberth and Dai 2007). Suppression of precipitation was also exhibited in numerical simulations with sulphur emissions in the stratosphere employing climate models of different complexity (Matthews and Caldeira 2007; Robock et al. 2008; Brovkin et al. 2009). In addition, sulphate particles in the stratosphere may enhance ozone destruction (Zerefos et al. 1994; Angell 1997; Solomon 1999). As a result, practical implementation of geoengineering would lead to the formation of ozone holes both in the Antarctic and in the Arctic (Tilmes et al. 2008).

If sulphur emissions in the stratosphere are employed but ceased after some time, e.g., due to the discovery of unexpected negative side effects or due to technological failure, Earth's climate would warm rapidly (Matthews and Caldeira 2007; Robock et al. 2008; Brovkin et al. 2009; Eliseev et al. 2009).

Moreover, the intensity of sulphur emissions in the stratosphere needed for practical implementation of geoengineering remains unclear. Even in the idealised case of the equilibrium climatic response to the doubled carbon dioxide in the atmosphere, estimations of this intensity differ by orders of magnitude, from ≈ 0.6 to 5 TgS/year (Izrael 2005; Crutzen 2006; Wigley 2006; Rasch et al. 2008a). In particular, Rasch et al. (2008a) have shown that the required intensity depends on the size of the particles, with small particles being more efficient in comparison to larger ones.

As a result, there is an ongoing debate on the efficiency and adequacy of the proposed geoengineering scheme. The goal of the present paper is to contribute to this discussion by estimating sulphur emissions in the stratosphere required to mitigate the global warming induced by the moderate scenario SRES A1B of anthropogenic influence in the twenty-first century. In addition, possible side effects are assessed.

One may consider a principal possibility to control sulphate particle size in the course of geoengineering. This would affect both radiative efficiency of the emitted sulphates and their residence time in the stratosphere. Additional complications arise due to possible nonspherical shapes of the stratospheric sulphur particles. As a result, in the present paper, ensemble numerical experiments with the climate model of intermediate complexity developed at the A.M. Obukhov Institute of Atmospheric Physics RAS (IAP RAS CM) are performed varying, in a systematic manner, values of different governing parameters related to the problem at hand. In this respect, the results presented in the paper differ from those published earlier by the other authors (see above).

Another feature distinguishing the present paper from those already published is related to the mitigation target. In other papers, either complete mitigation of the anthropogenically induced global warming is studied (e.g., Matthews and Caldeira 2007; Rasch et al. 2008a) or global warming is not allowed to exceed a prescribed threshold (Brovkin et al. 2009). In the present paper, we apply a strategy to limit the decadal scale temperature trend rather then the temperature itself. While, for a given time interval, the limiting trend result in limited global warming, these approaches are not equivalent. In particular, one may argue that terrestrial and oceanic ecosystems may adopt to slow climatic changes but would become vulnerable if these changes are fast. Influence of the temperature change rate on particular parts of the climate system was demonstrated earlier (Stocker and Schmittner 1997; Demchenko et al. 2006). In addition to this, we explore geoengineering efficiency in a globally averaged energy-balance climate model to further interpret the obtained results.

The present paper is a substantial extension of the papers on geoengineering mitigation of global warming recently published by the same authors (Chernokulsky et al. 2010; Eliseev and Mokhov 2009; Eliseev et al. 2009). In particular, about a half of the IAP RAS CM simulations presented here were not published elsewhere. All results concerning non-complete mitigation of global warming obtained with the IAP RAS CM and energy balance model (see below) are entirely new. The results concerning temperature and precipitation response to transient geoengineering mitigation (simulation ensemble GEOINT, see below) obtained under non-uniform latitudinal distributions of stratospheric sulphates were not published in regular journals as well. An application of the radiative efficacy concept of stratospheric sulphates (Hansen et al. 2005) for

geoengineering mitigation was also not pursued earlier. These issues motivated the authors to submit the present paper for publication.

2 Numerical model and performed simulations

In this work, the numerical climate model of intermediate complexity developed at the A.M. Obukhov Institute of Atmospheric Physics RAS (IAP RAS CM, version (Eliseev and Mokhov 2008, 2009; Mokhov et al. 2008a, b, c)) is used. Optical thickness of scattering stratospheric aerosols in the model depends linearly on their extinction coefficient $k_{e,a,st}$ and aerosol burden per unit area $m_{a,st}$

$$\tau_{a,st} = k_{e,a,st} m_{a,st}. \tag{1}$$

In turn, instantaneous radiative forcing at the top of the atmosphere

$$R_{a,st,\mathrm{TOA}} = -a_{a,st}\tau_{a,st} \tag{2}$$

with $a_{a,st} = 22\ \mathrm{W/m^2}$ (Hansen et al. 2005). The value of $k_{e,a,st}$ is estimated based on measurements performed for the aerosol loading after the Mt. Pinatubo eruption (1991). For this eruption, the total mass of sulphur injected in the atmosphere is estimated to be ≈ 10 TgS (Bluth et al. 1992) and $\tau_{a,st}$ reached 0.15 (Hansen et al. 1992). This leads to $k_{e,a,st} = 7.6\ \mathrm{m^2/g}$.

The IAP RAS CM with an implemented relationship (Eq. 2) has been validated against the observationally derived surface air temperature response on past volcanism (Eliseev and Mokhov 2008). In particular, the model realistically reproduces annual mean response to the major twentieth century volcanic eruptions.

Numerical experiments with the IAP RAS CM were performed for 1860–2100 forced by annual anthropogenic emissions of carbon dioxide and methane (which are converted to the respective atmospheric concentrations by the carbon and methane cycle modules of the model), by annual mean atmospheric concentrations of nitrogen peroxide and tropospheric sulphates, by annual mean sulphate concentrations in the troposphere, and by annual emissions of sulphates in the stratosphere.

In the numerical experiment ANTHRO, geoengineering mitigation is not applied. Anthropogenic emissions of CO_2 due to fossil fuel and land use are prescribed for 1860–2000 according to the data (Marland et al. 2005) and (Houghton 2003), respectively. Anthropogenic emissions of CH_4 for the eighteenth–twentieth centuries are adopted from (Stern and Kaufmann 1996) but reduced uniformly in time by 13% as described by Eliseev et al. (2008). All these emissions are continued in the twenty-first century according to the moderate SRES A1B scenario (Houghton et al. 2001). Historic atmospheric concentration of N_2O is prescribed based on the GISP2 borehole data (MacFarling Meure et al. 2006); for the twenty-first century, it is adopted from the BernCC simulations (Houghton et al. 2001) forced by the same SRES A1B scenario. Tropospheric sulphate burden is prescribed according to the historic+SRES A1B simulations with the model MOZART 2.0 (Horowitz 2006).

In the numerical experiments with geoengineering mitigation, global mass $M_{a,st,g}$ of the stratospheric aerosols is modelled via

$$\frac{dM_{a,st,g}}{dt} = E_{a,st,g} - \frac{M_{a,st,g}}{t_{a,st}}, \tag{3}$$

where t is time, $E_{a,st,g}$ is stratospheric sulphur emission per annum and $t_{a,st}$ stands for residence time of stratospheric aerosols. Based on fast mixing of volcanic aerosol clouds in zonal direction (Robock 2000), zonal distribution of resulting stratospheric sulphates is assumed to be homogeneous. As a result, local burden $m_{a,st}$ is prescribed employing latitudinal profile $Y(\phi)$ only (Mokhov and Eliseev 2008; Eliseev and Mokhov 2009; Eliseev et al. 2009)

$$m_{a,st} = \frac{M_{a,st,g}}{S_E} Y(\phi), \tag{4}$$

where S_E stands for the Earth's surface area. In the here-presented numerical experiments, three types of $Y(\phi)$ are explored: homogeneous distribution with $Y(\phi) \equiv 1/2$, triangular function of $x = \sin\phi$ with maximum at $x = x_0$ and respective trapezoidal function with plato at $-x_1 \le x \le x_1$ (see Fig. 1). In principle, such latitudinal profiles have to be conditioned by atmospheric dynamics (Rasch et al. 2008a; Robock et al. 2008). As a result, some of the imposed $Y(\phi)$ values may be unrealistic. However, it is still valuable to study an impact of different latitudinal distributions of stratospheric sulphates. One may argue that the latter may help to develop more efficient mitigation strategies.

Two sets of ensemble numerical experiments with geoengineering mitigation are performed in this paper. The first set, GEOCONST, consists of constant emissions between the starting year t_0 and the ending year t_1:

$$E_{a,st,g} = \begin{cases} E_0, & \text{if } t_0 \le t \le t_1 \\ 0, & \text{otherwise} \end{cases} : \qquad \text{GEOCONST.}$$

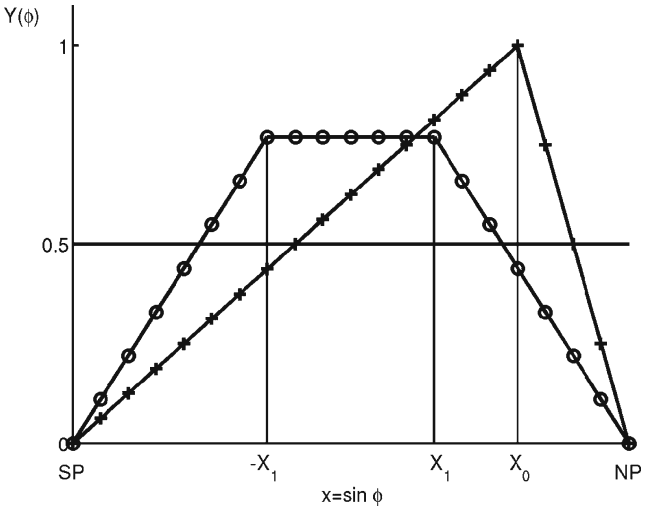

Fig. 1 Latitudinal distributions of stratospheric sulphates (expressed as functions of $x = \sin\phi$) used in the paper: uniform (*solid line*), triangular with maximum at $x = x_0$ (*pluses*), and trapezoidal with plato at $-x_1 \le x \le x_1$ (*circles*)

In the second set, GEOINT, emissions are set proportional to the top-of-the-atmosphere instantaneous radiative forcings imposed by the SRES A1B scenario:

$$E_{a,st,g} = \begin{cases} k_E R_{\mathrm{TOA,SRES\,A1B}}, & \text{if } t_0 \le t \le t_1 \\ 0, & \text{otherwise} \end{cases} : \text{GEOINT}$$

with $k_E = 0.3 - 10$ (TgS/year)/(W/m^2) depending on ensemble member.

In addition, ensemble members differ between each other by values of extinction coefficient, sulphate residence time in the stratosphere, latitudinal distribution and starting and ending years of applied emissions. In particular, extinction coefficient $k_{e,a,st}$ is varied from 5.0 to 10.0 m^2/g for the GEOINT ensemble. This choice is related to the uncertainty in stratospheric sulphur burden after the Mt. Pinatubo eruption, which declined within half a year from about 10 TgS (Bluth et al. 1992) to about 6 TgS (Hansen et al. 1992) and to the uncertainty of the empirically derived coefficient $a_{a,st}$, which, in different papers, is varied from 13 (Chou et al. 1984) to 30 W/m^2 (Lacis et al. 1992) (see also Stowe et al. 1992; Andronova et al. 1999; Hansen et al. 2005). Moreover, one may, in principle, consider a possibility to control effective radii of sulphate particles in the course of the geoengineering mitigation. Particles emitted during volcanic eruptions have typical radii of several hundred nanometres (Rasch et al. 2008a). If the Mie theory is applied, radiative efficiency of such particles correlates negatively with their sizes. Large particles with effective radii above about 0.3 μm, in addition to scattering solar radiation, also absorb in the longwave (Rasch et al. 2008a). The latter effect is ignored in our simulations because single scattering albedo of stratospheric sulphates is assumed to equal unity irrespective of wavelength in the IAP RAS CM. An even wider interval of $k_{e,a,st}$, from 5.0 to 20.0 m^2/g, is explored for the GEOCONST ensemble.

Residence time of stratospheric sulphates $t_{a,st}$ is varied from 2 to 3 years (Izrael 2005; Robock et al. 2008; Rasch et al. 2008a). Depending on ensemble members, the first year when sulphur is injected in the stratosphere is set either to A.D. 2015 or to A.D. 2040. In turn, applied emissions either stopped in year 2075 or continued up to year 2100. In addition, both the GEOCONST and GEOINT ensemble members differ between each other by choice of $Y(\phi)$ with different shape and positions either of x_0 or of x_1.

3 Geoengineering efficiency as simulated by the IAP RAS CM

3.1 Temperature changes in the numerical experiments without geoengineering mitigation

Temperature response in the experiment ANTHRO is described by Eliseev et al. (2007), where this simulation is denoted as GHGSA–A1B. Linear trend of the global surface air temperature T_g for the twentieth century in this experiment is 0.55 K in accordance with the observational data 0.6 ± 0.2 K (Trenberth et al. 2007). Global temperature increases by 3.0 **K** (2.4 **K**) with respect to the preindustrial state (late twentieth century). These values are in general agreement with the simulations performed with other climate models. In particular, the latter value falls within the range figured by the IPCC AR4 climate model ensemble under the same SRES A1B scenario, from 1.7 to 4.4 K with a mean value of 2.8 K (Meehl et al. 2007). In the IAP RAS CM, as well as in other climate models, surface air temperature (SAT) increases most markedly in the middle and high latitudes, especially over land. To the middle of the twenty-first century, extratropical SAT rises by 1–2 K over oceans and by 2–5 K over land. To the late twenty-first century, even in the tropics, the annual mean surface warming is above 1 K; in the extratropics, it is larger than 2 K, and over high latitude land, there are regions with warming >5 K (Fig. 2).

3.2 Dependence of mitigation efficiency on latitudinal distribution of stratospheric sulphates

As expected, global top-of-the-atmosphere instantaneous radiative forcing is larger for the latitudinal distributions $Y(\phi)$ with high loadings in the tropics.

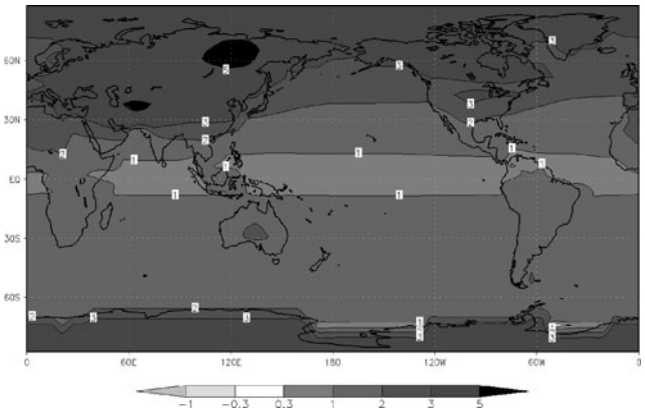

Fig. 2 Surface air temperature change (K) in 2091–2100 relative to 2000–2100 in the numerical experiment ANTHRO

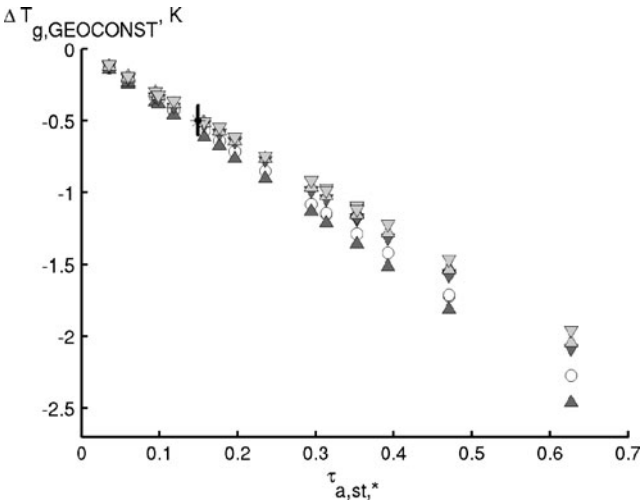

Fig. 3 Difference of T_g (K) in the late twenty first century between GEOCONST (ensemble members with mitigation continued up to year 2100) and ANTHRO vs $\tau_{a,st,*}$ (see Eq. 5) for the uniform (*circles*) latitudinal distribution of stratospheric sulphates $Y(\phi)$, the triangular distributions with maximum loadings either at $70°N$ or at $30°N$ (*directed upward dark* and *light gray triangles* correspondingly), and the trapezoidal distributions with a plato either in $30°S-30°N$ or in $50°S-50°N$ (*directed downward dark* and *light gray triangles* correspondingly). Larger slope of lines formed by the plotted symbols indicates larger mitigation efficiency of a given latitudinal distribution of stratospheric sulphates. In addition, observationally derived response (Wigley 2000) to the change of stratospheric scattering aerosol optical depth due to the Mt. Pinatubo eruption in 1991 (Hansen et al. 2005) is shown

However, response of T_g on geoengineering mitigation is larger either for the uniform $Y(\phi)$ or for the latitudinal distributions, which peaked in the northern middle to subpolar latitudes. Efficiency of different latitudinal distributions may be quantified via

$$\tau_{a,st,*} = \frac{k_{e,a,st} E_{a,st,g} t_{a,st}}{S_E}. \tag{5}$$

This variable is a globally averaged optical thickness for the uniform $Y(\phi)$. Slope of T_g response on controlled sulphur injection in the stratosphere vs $\tau_{a,st,*}$ is larger for more efficient latitudinal distributions in comparison to less efficient ones (Fig. 3). It appears that this slope and corresponding efficiency is largest for the triangular distributions with x_0 located between $50°N$ and $70°N$. Uniform $Y(\phi)$ is slightly less efficient. The least efficient distributions are those that peaked in the tropics. The slope of T_g vs $\tau_{a,st,*}$ differs between the most and the least efficient latitudinal distributions by one third.

Difference in climate efficiency of different latitudinal distributions is in contrast with respective difference in global instantaneous top-of-the-atmosphere radiative forcing imposed by stratospheric sulphates. Provided other parameters are equal, this forcing is slightly larger, for instance, for the triangular $Y(\phi)$ with $\phi_0 = 0°N$ than for the triangular latitudinal distribution with maximum at $70°N$. However, temperature response for a given global burden of stratospheric sulphates is larger for the former latitudinal distribution than for the latter one. Such difference in sensitivity to applied radiative forcing is in agreement with the results by Hansen et al. (1997), who noted that response to unit forcing increases when localisation of this forcing moves from lower to higher latitudes. One may note in this context that here-studied triangular $Y(\phi)$ peaked between $50°N$ and $70°N$ still exhibited substantial stratospheric aerosol burden in the tropical area. It could be speculated that narrower meridional distribution with a maximum in the same northern middle-to-subpolar latitudes but with a small loading in the tropics would be inefficient for geoengineering purposes. The reason for the slightly smaller efficiency of the uniform $Y(\phi)$ may be related to the large loadings in the polar regions, which are ineffective during the polar night.

3.3 Interactive mitigation of global warming

Based on the results of Section 3.2, GEOINT ensemble is performed only for the uniform $Y(\phi)$ and for the triangular latitudinal distributions of tropospheric sulphates with maximum at $70°N$ and $50°N$. After completing this ensemble simulation, the model output was linearly interpolated with respect to parameter k_E scaling sulphate emissions in the stratosphere. From the latter output, ensemble members are chosen, fulfilling the condition that linear trend of T_g in every decade of

the twenty-first century is smaller than some prechosen value: $dT_g/dt < S_g$.

For complete mitigation of global warming during the twenty-first century (e.g., for $S_g = 0$) and if the mitigation emissions are applied since $t_0 =$ A.D. 2015 and continued up to year 2100, one needs sulphur emissions in the stratosphere amounting to 5–17 TgS/year in year 2050 and 8–28 TgS/year in year 2100 (Fig. 4). The lower end of these estimations corresponds to the large values of stratospheric aerosol extinction coefficient and of residence time of sulphates in the stratosphere, 10.0 m^2/g and 3 years correspondingly. In agreement with the results of Section 3.2, the emissions required for the uniform $Y(\phi)$ are slightly larger than those required for triangular horizontal distributions of stratospheric sulphates peaked at the northern middle-to-subpolar latitudes. The required emissions simulated by the IAP RAS CM are larger than those simulated employing the CLIMBER-2.3 model (Brovkin et al. 2009). A possible reason for this is due to differences in applied scenarios of anthropogenic influence on climate during the twenty-first century. Another reason for this discrepancy may be related to plausible overestimation of the required stratospheric sulphur emissions by the IAP RAS CM (see Section 5). If $t_0 =$ A.D. 2040, the required emissions hardly differ from those corresponding to $t_0 =$ A.D. 2040 due to fast response of T_g to applied mitigation. Similar fast response is commonly observed after volcanic eruptions (Robock 2000).

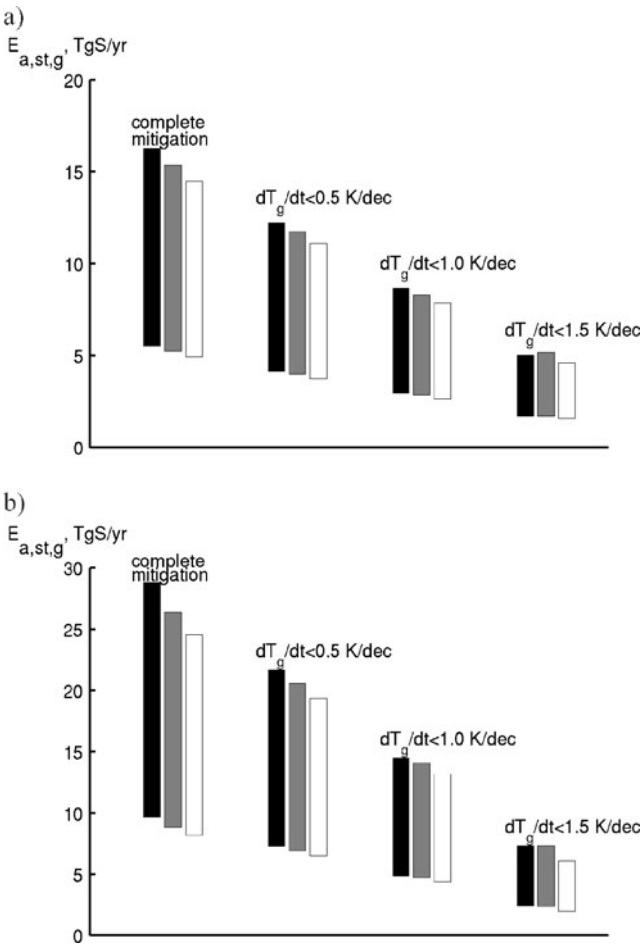

Fig. 4 Ranges of sulphur emissions (TgS/year) in the stratosphere required for complete compensation of global warming in the twenty-first century and for reducing the global temperature rise to 0.5 K/decade, to 1.0 K/decade, and to 1.5 K/decade (see labels) embedding here-studied values of aerosol extinction coefficients and their residence time in the stratosphere. Shown are the results for years 2050 (**a**) and 2100 (**b**) corresponding to the uniform horizontal distribution of sulphates in the stratosphere (*black bars*), and to the respective triangular distributions with a maximum either at 50° *N* (*gray bars*) or at 70° *N* (*white bars*)

Sulphur emissions in the stratosphere may be reduced if one needs to diminish the temperature trend in every decade of the twenty-first century to the value below $S_g \neq 0$ rather than to mitigate the warming completely. Particularly, if the allowed value $S_g = 0.05$ K/decade, the required emissions are 4–12 TgS/year in year 2050 and 6–22 TgS/year in year 2100 (Fig. 4). For the values $S_g = 0.10$ K/decade ($S_g =$ 0.15 K/decade), the respective ranges for year 2050 are 3–9 TgS/year (2–5 TgS/year) and the ranges for year 2100 amount to 4–14 TgS/year (2–7 TgS/year); see Fig. 4.

Generally, these emissions are not negligible compared to the current anthropogenic emissions of sulphates in the troposphere. The latter for the 1990s is estimated to be 72 ± 6 TgS/year (Smith et al. 2001). Taking into account that, after gravitational sedimentation from the stratosphere, aerosol particles would reside in the troposphere until being deposited to the surface, geoengineering emissions may markedly enhance the tropospheric aerosol pollution.

Even in the case of complete global warming mitigation, substantial anomalies of annual mean SAT T develop in different regions. Their magnitude basically increases with time in accordance with growth of the sulphur emissions in the stratosphere. The geographical pattern of these anomalies depends on latitudinal distribution of atmospheric sulphates.

For the uniform distribution, there are positive SAT anomalies over the northern land, amounting to >1 K in the late twenty-first century (Fig. 5a). These anomalies are compensated by negative anomalies of smaller magnitude covering the whole Southern Hemisphere. Similar anomalies of T were found during boreal winter by Brovkin et al. (2009) under the same uniform distribution of stratospheric sulphates. In the latter paper,

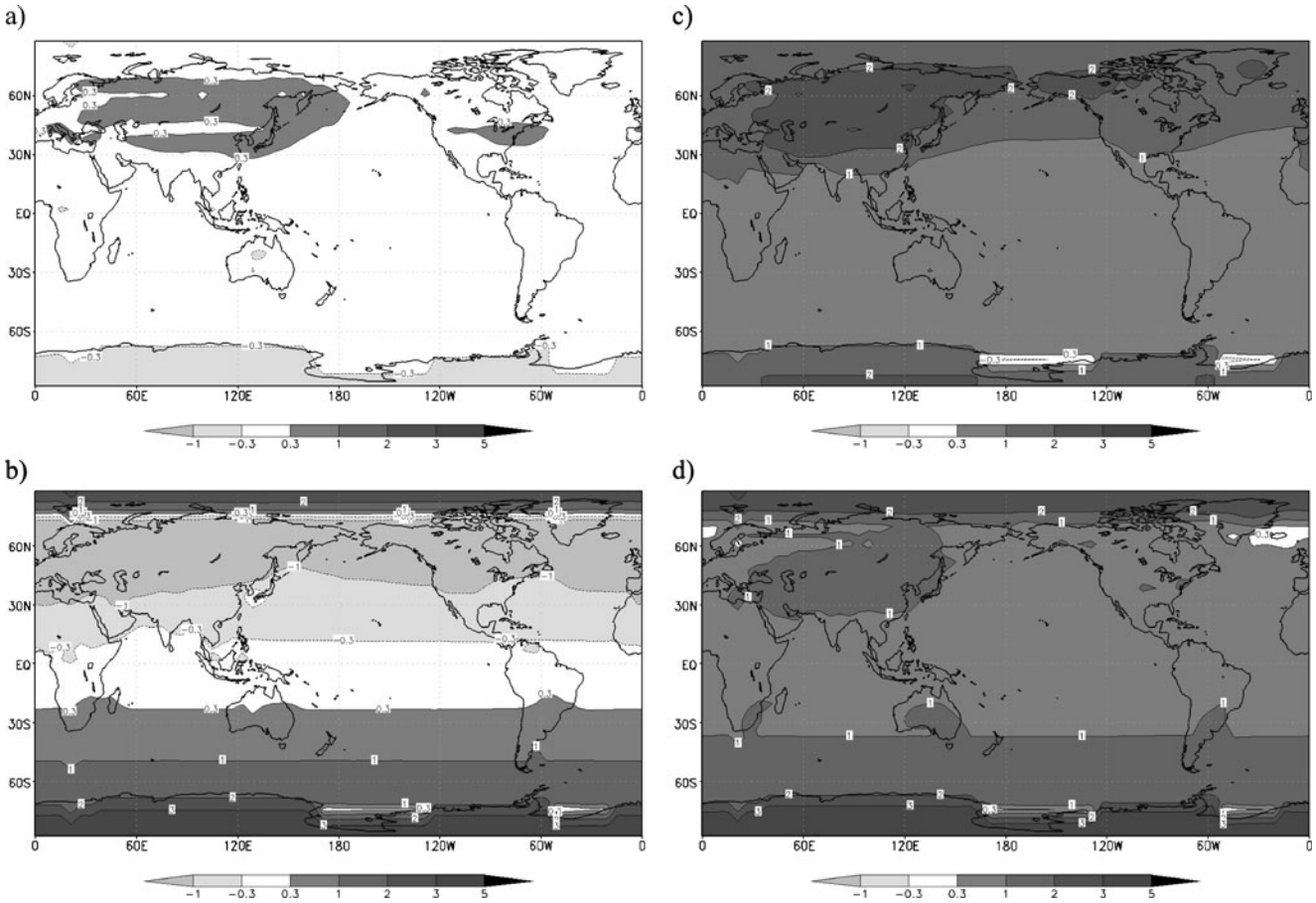

Fig. 5 Surface air temperature change (K) in 2091–2100 relative to 2000–2100 for the numerical experiments GEOINT. Shown are the case of complete global warming mitigation (**a**, **b**) and the case when linear trend of global temperature is not allowed to exceed 0.10 K/decade in the twenty-first century (**c**, **d**) for uniform $Y(\phi)$ (**a**, **c**) and triangular $Y(\phi)$ with $\phi_0 = 70^\circ N$ (**b**, **d**)

these anomalies are partly compensated by cooling developed during boreal summer. Annual mean warming of the order of about 1 K over the northern midlatitudinal land was also found in (Matthews and Caldeira 2007). However, the general pattern of SAT response to combined SRES A1B and geoengineering forcing in this paper differs from that obtained in our paper due to the absence of Antarctic warming, exhibited by Matthews and Caldeira (2007), in our results.

In contrast, if one selects the triangular distribution, warming over the northern land is mitigated excessively, with a cooling with a magnitude above 1 K in the northern midlatitudes (Fig. 5b). However, these negative anomalies are compensated by strong surface air positive anomalies in the Arctic and in the middle and high latitudes of the Southern Hemisphere. A positive SAT anomaly also develops near the east Asian coast related to the suppression of the summer South-Asian monsoon. In particular, the cooling induced by geoengineering is stronger in summer over the eastern part of Asia than over the adjacent ocean (not shown). This decreases the summer land–sea temperature contrast in this region and, therefore, suppresses the corresponding monsoon. In winter, the situation is reversed and the South-Asian monsoon is enhanced. In the annual mean, summer monsoon suppression dominates over winter enhancement (e.g., Fig. 5a) due to stronger geoengineering climatic forcing in summer. The latter is due to larger insolation in summer than in winter.

For both uniform and triangular latitudinal distributions, SAT response on geoengineering mitigation consists of anomalies of one sign in the northern middle latitudes and anomalies of another sign in the middle and subpolar latitudes of the Southern Hemisphere. This is related to the changes in intensity of the oceanic thermohaline circulation (THC). For the uniform $Y(\phi)$, positive temperature anomalies in the Northern Hemisphere and negative temperature anomalies in the

Antarctic imply stronger THC in comparison to the present-day state. In turn, widespread warming of the Southern Hemisphere and cooling of the northern tropical and middle latitudes suggest suppressed heat transport by oceanic currents for the case of triangular latitudinal distribution of stratospheric sulphates.

If $S_g \neq 0$, geoengineering mitigation still allows a substantial reduction in the warming. For the case $S_g = 0.10$ and for the uniform latitudinal distribution of stratospheric sulphates, T increases not larger than by 1 K in the tropics and over the southern extratropical oceans (Fig. 5c). Over other oceanic regions, warming does not exceed 2 K. Over extratropical land, the simulated annual mean SAT rise is below 3 K. This anomaly is additionally dampened for the case of triangular $Y(\phi)$ with a maximum in the high to subpolar latitudes (Fig. 5d) and does not exceed 2 K in the late twenty-first century. However, in the latter case, larger warming is simulated in the Arctic (2–3 K) and in the Antarctic (4–5 K). If $S_g = 0.15$ K/decade, warming over the extratropical latitudes is enhanced additionally and comes close to that simulated in the numerical experiment ANTHRO.

Globally averaged precipitation P_g decreases during the twenty-first century by 12–13 cm/year relative to 2000–2010 for the case of complete mitigation of global warming. Despite a very similar globally averaged value, geographical patterns of precipitation change differ between different $Y(\phi)$. For the uniform latitudinal distribution of stratospheric sulphates, annual precipitation decreases by 5–10 cm/year with respect to the first decade of the twenty-first century in the tropical areas and in the southern storm tracks (Fig. 6a). Similar precipitation response has been simulated by Brovkin et al. (2009). Marked reduction in precipitation over the tropical west Pacific as a response to the combined anthropogenic and geoengineering forcing was also simulated by Robock et al. (2008), and the reduction of precipitation over the near-equatorial continental areas under similar scenario was exhibited in (Matthews and Caldeira 2007).

For the case of complete global warming mitigation in the twenty-first century and for the triangular distribution of stratospheric sulphates peaked at 50° N or at 70° N, annual precipitation decreases by 5–10 cm/year relative to 2000–2010 in the northern subtropics (in particular, in the region of the South-Asian monsoon) and respectively increases by 5–10 cm/year in the southern storm tracks (Fig. 6b). The precipitation decrease in the south-east of Asia is in agreement with the suppression of summer monsoon there. Similar precipitation decrease was also simulated by Brovkin et al. (2009).

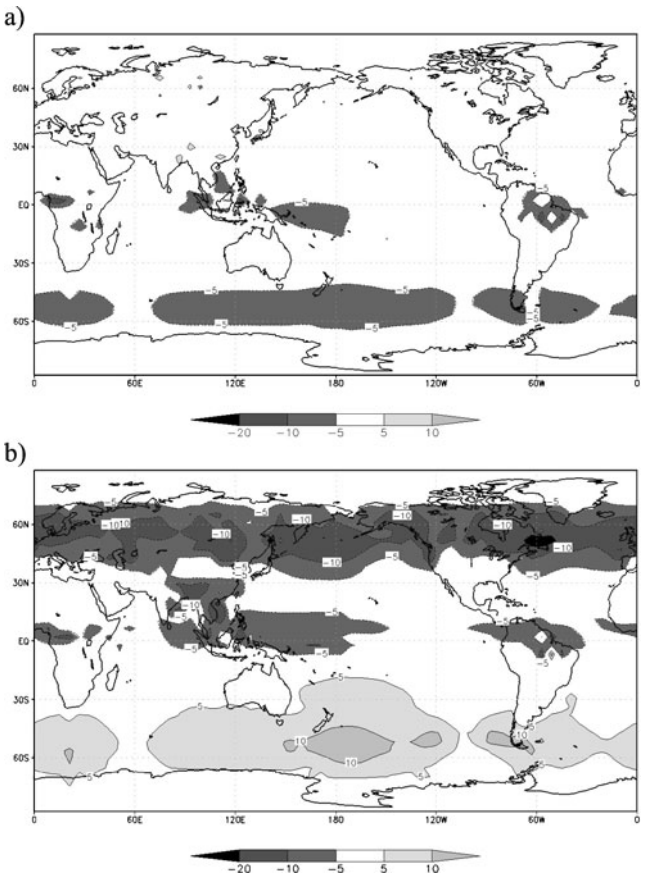

Fig. 6 Annual precipitation change (cm/year) in 2091–2100 relative to 2000–2100 for the numerical experiments GEOINT for the case of complete global warming mitigation for uniform $Y(\phi)$ (**a**) and triangular $Y(\phi)$ with $\phi_0 = 70° N$ (**b**)

3.4 Rapid temperature rise after the geoengineering ceases

If geoengineering proceeds for a finite time interval and ceases afterwards, a large disparity between the applied radiative forcing and current state of the climate system develops. As a result, global temperature starts to evolve rapidly to the curve corresponding to the imposed SRES A1B scenario (Fig. 7). A few decades after the geoengineering emission stops in 2075, T_g comes close to the global temperature curve simulated in the numerical experiment ANTHRO. During the decade 2076–2085, global temperature increases by 0.6–1.5 K depending on S_g. In the decade 2086–2075, T_g rises by another ≈ 0.2 K.

Even larger SAT changes occur after the geoengineering stops at the regional level. For complete miti-

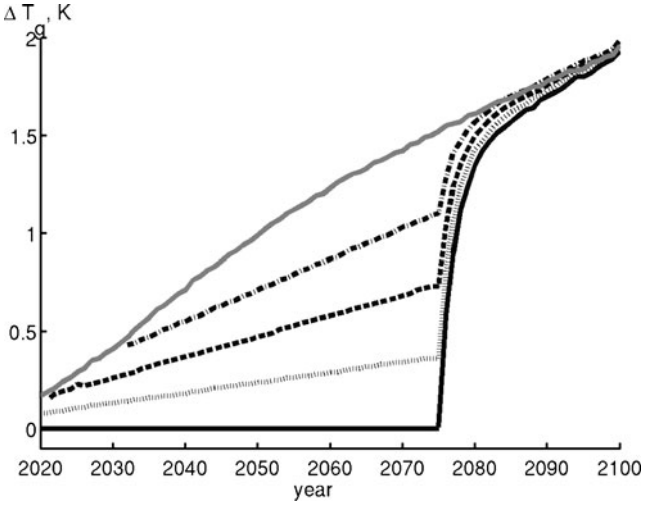

Fig. 7 Global temperature change relative to 2001–2010 if the geoengineering emissions are stopped in year 2075 for complete global warming mitigation prior to this year (*black solid line*), $S_g = 0.05$ K/decade (*dotted curve*), $S_g = 0.10$ K/decade (*dashed line*), $S_g = 0.15$ K/decade (*dashed–dotted line*) in comparison with the results of the ANTHRO experiment (*gray line*). All curves (except ANTHRO) correspond to $k_{e,a,st} = 7.6$ m^2/g, $\tau_{a,st} = 2.5$ year, and to the uniform horizontal distribution of stratospheric sulphates. Curves for other settings of these three parameters practically indistinguishable from those drawn in this figure

gation of the SRES A1B-induced warming, they could be as large as 3 K/decade in the interiors of Eurasia and North America for the uniform latitudinal distribution of stratospheric sulphates, and even up to 5 K/decade for the triangular $Y(\phi)$ with a maximum at $70^\circ N$ (Fig. 8a, b). These values can be compared with the regional SAT changes during the same decade 2076–2085 obtained in the ANTHRO experiment, which are not larger than 0.7 K/decade. In contrast to the uniform $Y(\phi)$, the respective triangular distribution peak in middle-to-subpolar northern latitudes does not lead to strong warming in the Arctic and Antarctic during the decade 2076–2085.

Again, this negative consequence of geoengineering may be moderated if $S_g > 0$ is allowed in the twenty-first century. However, even for the rather large value $S_g = 0.15$ K/decade, SAT rise amounts to 2 K/decade in the Eurasian and North American interiors for the uniform $Y(\phi)$ and up to 3 K/decade in the same regions for the triangular $Y(\phi)$ peaked either at $50^\circ N$ or at $70^\circ N$.

Rapid—with a timescale of a few decades—removal of the temperature effect of geoengineering after the respective emission stop was also exhibited in Matthews and Caldeira (2007), Robock et al. (2008), Brovkin et al. (2009).

4 Results obtained with an energy-balance model

To explore further geoengineering climate mitigation, one may employ a globally averaged energy balance model, which reads

$$C\frac{dT_g}{dt} = F_{\mathrm{TOA}}, \tag{6}$$

where C stands for effective heat capacity of the system per unit area and F_{TOA} is radiative budget at the top of the atmosphere. Considering the present-day state (hereafter denoted by the subindex "0") and the future basic state differing from the present-day one by global temperature ΔT_g, one obtains

$$C\frac{d\Delta T_g}{dt} = F_{\mathrm{TOA}} - F_{\mathrm{TOA},0} + C\left(\frac{dT_g}{dt}\right)_0. \tag{7}$$

Expanding the term $F_{\mathrm{TOA}} - F_{\mathrm{TOA},0}$ as a sum of forcing R and linear feedback $-\lambda\Delta T_g$, one gets

$$C\frac{d\Delta T_g}{dt} = F - \lambda\Delta T_g + C\left(\frac{dT_g}{dt}\right)_0. \tag{8}$$

Here, climate sensitivity is $\lambda = R_{2\times CO_2}/\Delta T_{g,2\times CO_2}$, $R_{2\times CO_2}$ stands for radiative forcing corresponding to the doubled CO_2 content in the atmosphere and $\Delta T_{g,2\times CO_2}$ is corresponding equilibrium response of temperature.

The solution of Eq. 8 reads

$$\Delta T_g = \frac{1}{C}e^{-\lambda t/C}\int_0^t R(\xi)e^{\lambda t/C}\,d\xi + \left(\frac{dT_g}{dt}\right)_0\frac{C}{\lambda}\left(1-e^{-\lambda t/C}\right), \tag{9}$$

where $t = 0$ corresponds to the present day. Equation 9 leads to

$$\frac{d\Delta T_g}{dt} = -\frac{\lambda}{C^2}e^{-\lambda t/C}\int_0^t R(\xi)e^{\lambda t/C}\,d\xi + \frac{1}{C}R(t) + \left(\frac{dT_g}{dt}\right)_0 e^{-\lambda t/C}. \tag{10}$$

One may simplify the problem considering only the forcing due to anthropogenic greenhouse gases $R_{\mathrm{GHG},g}$ and the forcing due to stratospheric sulphates $R_{a,st,g}$. The former may be expressed via change of the equiv-

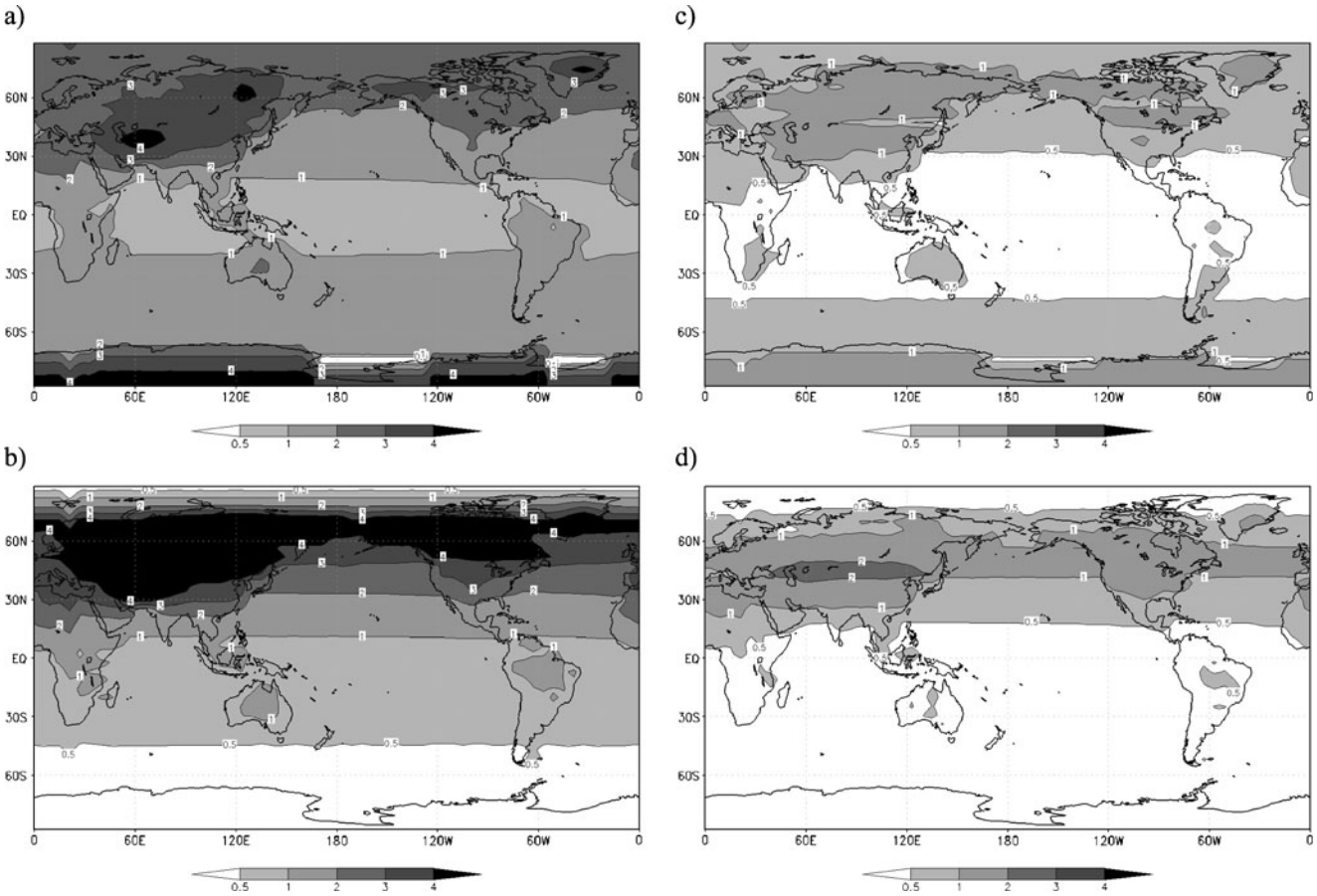

Fig. 8 Surface air temperature change (K) in 2076–2085 in the numerical experiments GEOINT if geoengineering emissions are ceased in 2075. Shown are the case of complete global warming mitigation (**a**, **b**) and the case when linear trend of global temperature is not allowed to exceed 0.15 K/decade in the twenty-first century (**c**, **d**) for uniform $Y(\phi)$ (**a**, **c**), triangular $Y(\phi)$ with $\phi_0 = 70^\circ N$ (**b**) and triangular $Y(\phi)$ with $\phi_0 = 50^\circ N$ (**d**)

alent CO_2 atmospheric content (Myhre et al. 1998), q_{GHG}, as follows:

$$R_{\mathrm{GHG},g} = \frac{R_{2\times CO_2}}{\ln 2} \exp\left(\frac{q_{\mathrm{GHG}}}{q_{\mathrm{GHG},0}}\right).$$

Top-of-the-atmosphere radiative forcing due to stratospheric sulphates is written in a fashion similar to that used in the IAP RAS CM (see Eqs. 1 and 2). However, because energy-balance model lacks vertical resolution and resulting dependence of climate sensitivity on forcing agent, stratospheric aerosol forcing is multiplied by the efficacy factor α with respect to the forcing due to anthropogenic greenhouse gases (Hansen et al. 2005)

$$R_{a,st,g} = -\alpha a k_e a, stM_{a,st,g}/S_E.$$

To make the problem more tractable, Eq. 3 is replaced by

$$M_{a,st,g} = E_{a,st,g} t_{a,st},$$

which follows from Eq. 3 in a stationary approximation (Chernokulsky et al. 2010). Further, equivalent CO_2 content in the atmosphere is assumed to depend on time exponentially

$$q_{\mathrm{GHG}} = q_{\mathrm{GHG},0} \exp\left(t/t_p\right),$$

with characteristic time t_p. In this case, $R_{\mathrm{GHG},g} = \left(R_{2\times CO_2}/\ln 2\right) t/t_p$. Assume also that $E_{a,st,g}$ linearly increases in time with a rate e_0. As a result,

$$R = gt,$$

with

$$g = \frac{R_{2\times CO_2}}{t_p \ln 2} - \frac{\alpha e_0 a k_{e,a,st} t_{a,st}}{S_E}.$$

In this case, Eq. 10 may be reduced to

$$\frac{d\Delta T_g}{dt} = \frac{g}{\lambda}\left(1 + e^{-\lambda t/C}\right) + \left(\frac{dT_g}{dt}\right)_0 e^{-\lambda t/C}.$$

It follows from the latter equation that $d\Delta T_g/dt \le S_g$ if

$$g \le \lambda \frac{S_g - \left(dT_g/dt\right)_0 e^{-\lambda t/C}}{1 + e^{-\lambda t/C}}$$

or

$$E_{a,st,g} \ge \frac{S_E t}{\alpha a k_{e,a,st} t_{a,st}} \left[\frac{R_{2\times CO_2}}{t_p \ln 2} - \lambda \frac{S_g - \left(dT_g/dt\right)_0 e^{-\lambda t/C}}{1 + e^{-\lambda t/C}} \right]. \quad (11)$$

Computations with the energy-balance model are performed for $C = 1.1 \times 10^9\ J\,m^{-2}\,K^{-1}$ (Andreae et al. 2005) and $R_{2\times CO_2} = 3.7\ W\,m^{-2}$ (Meehl et al. 2007). The present-day global SAT tendency is set to 0.17 K/decade (Trenberth et al. 2007). In addition, to explore an influence of the present-day climate non-stationarity on obtained results, the case $\left(dT_g/dt\right)_0 = 0$ is studied as well. Stratospheric sulphates radiative efficacy α is set either to 0.8 (Hansen et al. 2005) or to unity. The latter case corresponds to the neglect of the influence of vertical structure of the imposed radiative forcing on geoengineering efficiency. Equilibrium climate sensitivity to the doubling of the carbon dioxide atmospheric content is varied from 2.0 to 4.5 K (Meehl et al. 2007). Time scale t_p is varied from 50 to 250 years, which are characteristic of the SRES scenario family (Chernokulsky et al. 2010). Stratospheric aerosol extinction coefficient and their residence time in the stratosphere are varied within the same ranges as it was for the IAP RAS CM.

Complete mitigation of the greenhouse-gas-induced warming requires 6–8 TgS/year in year 2100 in the

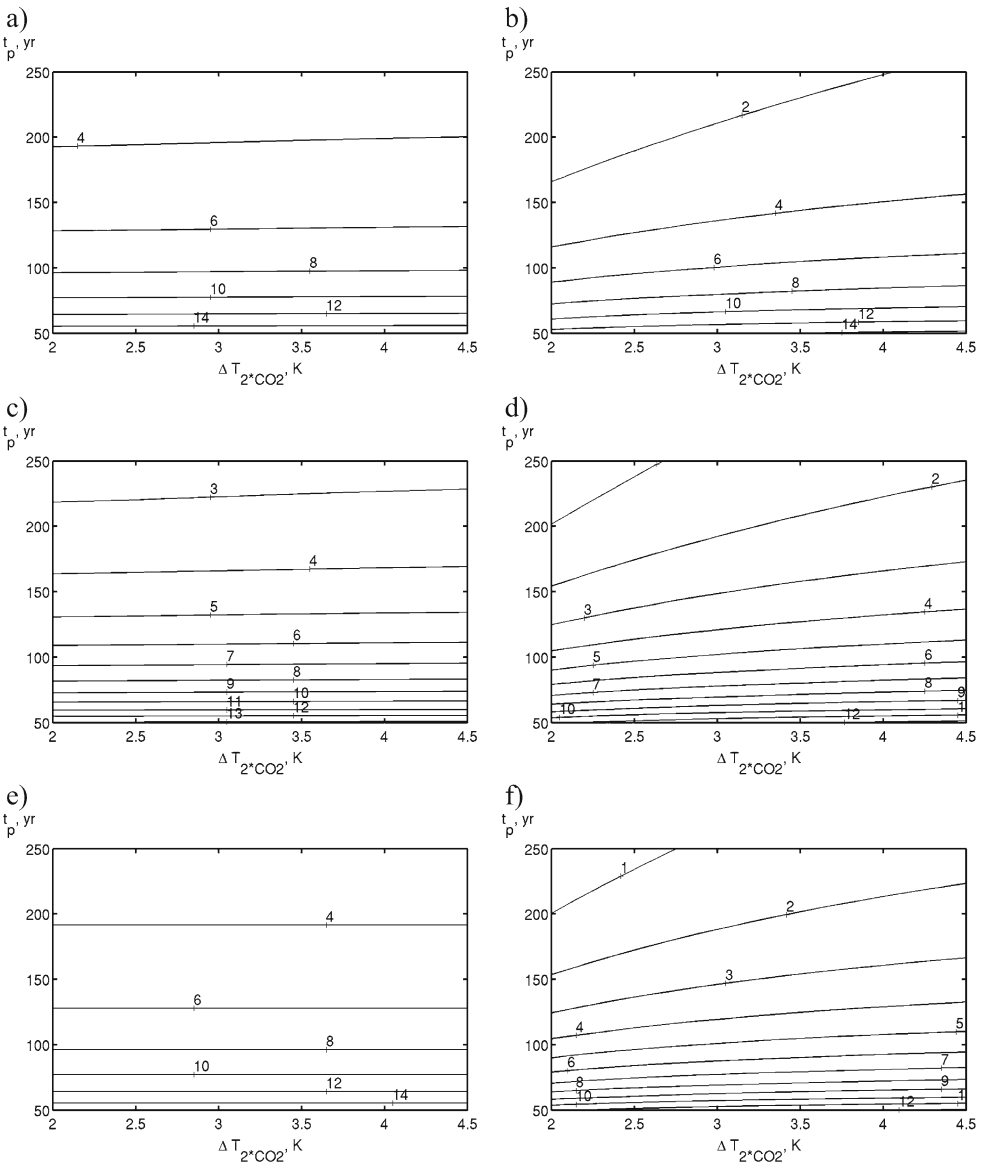

Fig. 9 Emissions needed in year 2100 for complete compensation (**a**, **c**, **e**) of the greenhouse-gas indiced warming in the energy-balance climate model and to prevent the temperature rise from exceeding 0.1 K/decade (**b**, **d**, **f**) as a function of $\Delta T_{g,2\times CO_2}$, an equilibrium climate sensitivity to doubling of the atmospheric carbon dioxide content, and t_p, a time scale of the CO_2 atmospheric content growth. Shown are the cases $\left(dT_g/dt\right)_0 = 0.17$ K/decade, $\alpha = 0.85$ (**a**, **b**), $\left(dT_g/dt\right)_0 = 0.17$ K/decade, $\alpha = 1$ (**c**, **d**) and $\left(dT_g/dt\right)_0 = 0, \alpha = 0.8$ (**e**, **f**)

case when $\left(dT_g/dt\right)_0 = 0.17$ K/decade, $\alpha = 0.85$ and $t_p = (130–140)$ years. The latter range of t_p is characteristic of the SRES A1B scenario (Chernokulsky et al. 2010); see Fig. 9a. Emissions required for complete mitigation are almost independent from $\Delta T_{g,2\times CO_2}$. These emissions are smaller than those simulated by the IAP RAS CM. The reason for this discrepancy is due to neglect of the tropospheric sulphates in the energy-balance model, neglect of larger-than-unity radiative efficacy of non-CO_2 anthropogenic greenhouse gases (e.g., the climatic efficacy for methane is about 1.15 Hansen et al. 2005), and, most likely, from temporal dependence of effective heat capacity on time. The latter results from saturation of oceanic heat uptake as warming progresses (Hansen et al. 1985) and is difficult to explore in the context of the energy-balance model used here. In addition, a nonstationarity in Eq. 3 is neglected in the present model. However, the latter changes the stratospheric sulphates emissions required for mitigation by the value that is not larger than a few per cent in the late twenty-first century (Chernokulsky et al. 2010).

Neglect of difference in climatic efficacy between carbon dioxide and stratospheric sulphates results in even smaller, overly optimistic estimations for the required emissions. If $\left(dT_g/dt\right)_0 = 0.17$ K/decade and $t_p = (130–140)$ years, the required value is $E_{a,st,g} =$ 4–5 TgS/year (Fig. 9c). In contrast, neglect of the present day nonstationarity (setting $\left(dT_g/dt\right)_0 = 0$, Fig. 9e) hardly affects the required emissions except if $\Delta T_{g,2\times CO_2}$ is above about 3.5 K.

If $S_g > 0$ is allowed, the required emissions become smaller and depend on $\Delta T_{g,2\times CO_2}$ (Fig. 9b, d, f). For $\left(dT_g/dt\right)_0 = 0.17$ K/decade and $\alpha = 0.8$ ($\alpha = 1$) the estimated value of $E_{a,st,g}$ amounts to 3–5 TgS/year (3–4 TgS/year) if $t_p = (130–140)$ years and $S_g = 0.1$ K/decade.

For more aggressive anthropogenic scenarios with lower t_p, the required emissions increase. In particular, if t_p is about 100 years, which is characteristic of the SRES A2 scenario (Chernokulsky et al. 2010), the required emissions for the nonstationary present day state and climatic efficacy of the stratospheric sulphates $\alpha = 0.8$ are 8–10 Tg/year for complete mitigation and 6–8 TgS/year for $S_g = 0.1$ K/decade.

5 Summary and discussion

In this paper, a large ensemble of numerical experiments with the climate model of intermediate complexity developed at the A.M. Obukhov Institute of Atmospheric Physics RAS (IAP RAS CM) is performed to explore an efficiency of global warming mitigation via sulphate aerosol injection in the stratosphere. Different members of this ensemble are constructed by varying values of the parameters governing mass, horizontal distribution and radiative forcing of the stratospheric sulphates.

It was obtained that, among the here-studied latitudinal distributions $Y(\phi)$ of stratospheric sulphates, globally averaged instantaneous radiative forcing at the top of the atmosphere is maximum for those $Y(\phi)$ that peak in the tropics. However, the most efficient latitudinal distributions of the stratospheric sulphates are those that peak in the northern middle to subpolar latitudes. Uniform horizontal distribution of the stratospheric sulphates, frequently used in the geoengineering simulations, is slightly less efficient. These results are in general agreement with those exhibited by Hansen et al. (1997).

For complete mitigation of global warming developing under the moderate SRES A1B scenario of anthropogenic influence, one needs to emit 5–17 TgS/year (8–28 TgS/year) in the mid-twenty-first century (late twenty-first century) depending on the values of the above mentioned governing parameters. These emissions may be reduced if some warming is allowed to occur in the twenty-first century. For instance, if the global temperature trend S_g in every decade of this century is limited not to exceed 0.10 K/decade (0.15 K/decade), sulphur emissions in the stratosphere of 4–14 TgS/year (2–7 TgS/year) would be sufficient. Generally, these emissions are not a negligibly small part of the contemporary anthropogenic emissions of sulphate aerosol precursors.

Even in the case of the complete mitigation of global warming, mutually compensating SAT anomalies develop with a magnitude of about 1 K in the late twenty-first century in different regions. The pattern of these anomalies depends on the imposed latitudinal distribution of stratospheric sulphates. Even larger regional-scale anomalies simulated if $S_g > 0$ are allowed. When limitation on S_g is relaxed, these anomalies approach those simulated in the run without a geoengineering mitigation.

Application of geoengineering in the case of complete mitigation of globally averaged warming results in decrease of global precipitation by about 10% relative to the mean value for 2000–2010. In absolute units, the largest decrease of annual precipitation is simulated in the tropics and in the Southern Hemisphere storm tracks. This agrees with empirical and model-based studies (Groisman 1985; Trenberth and

Dai 2007; Matthews and Caldeira 2007; Robock et al. 2008; Brovkin et al. 2009).

If geoengineering sulphur emissions are applied for several decades and ceased afterwards, this leads to a rapid rise of SAT with an unprecedent rate that would amount to 5 K/decade in the interiors of Eurasia and North America.

These and other (see above) modelling results show that undesirable side effects of the proposed approach of geoengineering would be substantial in its practical implementation. Relatively large emissions of sulphur in the stratosphere would result in a marked enhancement of the tropospheric aerosol pollution due to eventual gravitational sedimentation of aerosol particles from the stratosphere to the troposphere. Even if the geoengineering succeeds on the global scale, it may be inefficient regionally. One notes that all the here-studied latitudinal distributions of stratospheric sulphates lead to regional SAT anomalies located either over the densely populated northern continents or in the high latitudes. This basically disqualifies the geoengineering target. Precipitation decrease in the Amazon and Congo valleys may trigger a dieback of tropical forests with corresponding suppression of carbon uptake from the atmosphere (see, e.g., Cox et al. 2004; Huntingford et al. 2004) and, respectively, an additional greenhouse warming. The latter, in turn, would require additional sulphur emissions to mitigate this warming. Rapid temperature rise occurring in the boreal regions after the geoengineering stops would pose a stress on the corresponding ecosystems. As these ecosystems are also important contributors to the carbon uptake from the atmosphere (e.g., Shvidenko and Nilsson 2003; Bonan 2008), this would also result in additional warming and, in turn, in additional sulphur emissions required to mitigate this warming.

The results obtained with the IAP RAS CM are further interpreted employing a globally averaged energy-balance climate model. It is shown that effective vertical localisation of the imposed radiative forcing is important for geoengineering efficiency. In agreement with (Hansen et al. 1997, 2005), this efficiency is diminished by about 15% due to localisation of the geoengineering forcing in the stratosphere in comparison to the carbon dioxide radiative forcing, which is effectively localised in the troposphere. This implies some caution concerning the results of emissions required for climate mitigations obtained with climate models lacking vertical resolution. In the latter case, the respective estimated emissions may be underestimated.

An importance of vertical localisation of the applied forcing for geoengineering efficiency may have some application for the IAP RAS CM as well. As mentioned above, the forcing due to stratospheric sulphates is applied at the top of the atmosphere while, in reality, it is expected to be localised in the lower stratosphere (Rasch et al. 2008b). As a result, the emissions required to mitigate global warming at different S_g would be overestimated somewhat in the present paper. However, we expect that this overestimation is not large. Moreover, other side effects of geoengineering, being consistent with other studies, are expected to depend only slightly on such localisation and robust provided forcing magnitude is fixed.

The basic results of the present paper are entirely new. As stated in Section 1, they are related to the influence of latitudinal distributions of stratospheric sulphates on emerging temperature and precipitation patterns, to estimation of required aerosol emissions in the case of incomplete mitigation of global warming and to application of the radiative efficacy concept for geoengineering mitigation issue. In turn, some results of the paper were simulated earlier by other groups employing different models. These results concern precipitation reduction due to geoengineering, spatial inhomogeneity of respective temperature mitigation and rapid removal of temperature mitigation after geoengineering emissions cease (see above). The results published here are in line with these publications. It is important to grow the body of evidence on side effects of the proposed geoengineering scheme taking into account possible concerns of its practical implementation.

Acknowledgements The authors are indebted to I.L. Karol and G.L. Stenchikov for useful discussions on the topic of the manuscript. Constructive comments of the anonymous reviewers were very helpful in improving the paper. This work has been supported by the Russian Foundation for Basic Research (grants 07-05-00164, 07-05-00273, 08-05-00358, 08-05-00532 and 09-05-13538), the President of Russia grant 755.2008.5 and the Programs of the Russian Ministry for Science and Education, Russian Federal Agency for Science and Innovations and the Russian Academy of Sciences.

References

Andreae MO, Jones CD, Cox PM (2005) Strong present-day aerosol cooling implies a hot future. Nature 435:1187–1190

Andronova NG, Rozanov EV, Yang F, Schlesinger ME, Stenchikov GL (1999) Radiative forcing by volcanic aerosols from 1850 to 1994. J Geophys Res 104:16807–18826

Angell JK (1997) Estimated impact of Agung, El Chichón, and Pinatubo volcanic eruptions on global and regional total ozone after adjustment for the QBO. Geophys Res Lett 24:647–650

Bluth GJS, Doiron SD, Schnetzler CC, Krueger AJ, Walter LS (1992) Global tracking of the SO2 clouds from the June, 1991

Mount Pinatubo eruptions. Geophys Res Lett 19:151–154. doi:10.1029/91GL02792
Bonan GB (2008) Forests and climate change: forcings, feedbacks, and the climate benefits of forests. Science 320:1444–1449
Brovkin V, Petoukhov V, Claussen M, Bauer E, Archer D, Jaeger C (2009) Geoengineering climate by stratospheric sulfur injections: earth system vulnerability to technological failure. Clim Change 92:243–259
Budyko MI (1977) Climate changes. American Geophysical Union, Washington, D.C., pp 244
Chernokulsky AV, Eliseev AV, Mokhov II (2010) Analytic estimations for efficiency of prevention of global warming by sulphur aerosol emissions into stratosphere. Rus Meteorol Hydrol, 35 (in press)
Chou M-D, Peng L, Arking A (1984) Climate studies with a multilayer energy balance model. Part III: climatic impact of stratospheric volcanic aerosols. J Atmos Sci 41:759–767
Cox PM, Betts RA, Collins M, Harris PP, Huntingford C, Jones CD (2004) Amazonian forest dieback under climate–carbon cycle projections for the 21st century. Theor Appl Climatol 78:137–156
Crutzen PJ (2006) Albedo enhancement by stratospheric sulfur injections: a contribution to resolve a policy dilemma? Clim Change 77:211–219
Demchenko PF, Eliseev AV, Arzhanov MM, Mokhov II (2006) Impact of global warming rate on permafrost degradation. Izv, Atmos Ocean Phys 42:32–39
Eliseev AV, Mokhov II (2008) Influence of volcanic activity on climate change in the past several centuries: assessments with a climate model of intermediate complexity. Izv, Atmos Ocean Phys 44:671–683
Eliseev AV, Mokhov II (2009) Model estimations of global warming mitigation efficiency depending on scenarios of controlled aerosol emissions in the stratosphere. Izv, Atmos Ocean Phys 45:221–232
Eliseev AV, Mokhov II, Arzhanov MM, Demchenko PF, Denisov SN (2008) Interaction of the methane cycle and processes in wetland ecosystems in a climate model of intermediate complexity. Izv, Atmos Ocean Phys 44:139–152
Eliseev AV, Mokhov II, Karpenko AA (2007) Influence of direct sulfate-aerosol radiative forcing on the results of numerical experiments with a climate model of intermediate complexity. Izv, Atmos Ocean Phys 42:544–554
Eliseev AV, Mokhov II, Karpenko AA (2009) Global warming mitigation by means of controlled aerosol emissions of sulphate aerosols into the stratosphere: global and regional peculiarities of temperature response as estimated in IAP RAS CM simulations. Atmos Ocean Opt 22:388–395
Groisman PYa (1985) Regional climatic consequences of volcanic eruptions. Soviet Meteorol Hydrol 10:39–45
Hansen J, Lacis A, Ruedy R, Sato M (1992) Potential climate impact of Mount Pinatubo eruption. Geophys Res Lett 19:215–218
Hansen J, Russell G, Lacis A, Fung I, Rind D, Stone P (1985) Climate response times: dependence on climate sensitivity and ocean mixing. Science 229:857–859
Hansen J, Sato M, Ruedy R (1997) Radiative forcing and climate response. J Geophys Res 102:6831–6864
Hansen J, Sato M, Ruedy R, Nazarenko L, Lacis A, Schmidt GA, Russell G, Aleinov I, Bauer M, Bauer S, Bell N, Cairns B, Canuto V, Chandler M, Cheng Y, Del Genio A, Faluvegi G, Fleming E, Friend A, Hall T, Jackman C, Kelley M, Kiang N, Koch D, Lean J, Lerner J, Lo K, Menon S, Miller R, Minnis P, Novakov T, Oinas Ja, Vand Perlwitz, Perlwitz Ju, Rind D, Romanou A, Shindell D, Stone P, Sun S, Tausnev N, Thresher D, Wielicki B, Wong T, Yao M, Zhang S (2005) Efficacy of climate forcings. J Geophys Res 110:D18104. doi:10.1029/2005JD005776
Hegerl GC, Zwiers FW, Braconnot P, Gillett NP, Luo Y, Marengo Orsini JA, Nicholls N, Penner JE, Stott PA (2007) Understanding and attributing climate change. In: Solomon S, Qin D, Manning M, Marquis M, Averyt K, Tignor MMB, LeRoy Miller H, Chen Z (eds) Climate change: the physical science basis. Cambridge University Press, Cambridge, pp 663–745
Horowitz LW (2006) Past, present, and future concentrations of tropospheric ozone and aerosols: methodology, ozone evaluation, and sensitivity to aerosol wet deposition. J Geophys Res 111:D22211. doi:10.1029/2005JD006937
Houghton JT, Ding Y, Griggs DJ, Noguer M, Linden van der PJ, Dai X, Maskell K, Johnson CA (eds) (2001) Climate change 2001: the scientific basis. contribution of working group I to the third assessment report of the intergovernmental panel on climate change. Cambridge University Press, Cambridge, pp 881
Houghton RA (2003) Revised estimates of the annual net flux of carbon to the atmosphere from changes in land use and land management 1850–2000. Tellus 55B:378–390
Huntingford C, Harris PP, Gedney N, Cox PM, Betts RA, Marengo JA, Gash JHC (2004) Using a GCM analogue model to investigate the potential for Amazonian forest dieback. Theor Appl Climatol 78:177–185
Izrael YuA (2005) An efficient way to regulate global climate is the main goal of the climate problem solution. Rus Meteorol Hydrol 30:1–4
Lacis A, Hansen J, Sato M (1992) Climate forcing by stratospheric aerosols. Geophys Res Lett 19:1607–1610
MacFarling Meure C, Etheridge D, Trudinger C, Steele P, Langenfelds R, Ommen van T, Smith A, Elkins J (2006) Law dome CO_2, CH_4 and N_2O ice core records extended to 2000 years BP. Geophys Res Lett 33:L14810. doi:10.1029/2006GL026152
Marland G, Boden TA, Andres RJ (2005) Global, regional, and national CO2 emissions. In: Trends: a compendium of data on global change. Carbon Dioxide Information Analysis Center Oak Ridge National Laboratory, U.S. Department of Energy, Oak Ridge, Tenn
Matthews HD, Caldeira K (2007) Transient climate–carbon simulations of planetary geoengineering. Proc Nat Acad Sci 104:9949–9954
Meehl GA, Stocker TF, Collins WD, Friedlingstein P, Gaye AT, Gregory JM, Kitoh A, Knutti R, Murphy JM, Noda A, Raper SCB, Watterson IG, Weaver AJ, Zhao Z-C (2007) Global climate projections. In: Solomon S, Qin D, Manning M, Marquis M, Averyt K, Tignor MMB, LeRoy Miller H, Chen Z (eds) Climate change 2007: the physical science basis. Cambridge University Press, Cambridge, pp 747–845
Mokhov II, Bezverkhnii VA, Eliseev AV, Karpenko AA (2008a) Model estimations of possible climatic changes in 21st century at different scenarios of solar and volcanic activities and anthropogenic impact. Cosmic Res 46:354–357
Mokhov II, Bezverkhny VA, Eliseev AV, Karpenko AA (2008b) Solar activity and estimation of its influence on global temperature. In: Zherebtsov GA (ed) Changes of natural environment and climate: natural and possible consequent human-induced catastrophes, v.VIII, solar activity and physical processes in the sun–earth system. ISTP SB RAS, Moscow, pp 143–149 (in Russian)

Mokhov II, Eliseev AV (2008) Geoengineering efficiency: preliminary assessment with a climate model of intermediate complexity. In: Côté J (ed) Research activities in atmospheric and oceanic modelling, vol WGNE Rep 38. World Climate Research Programme, Geneva, pp 07.21–07.22

Mokhov II, Eliseev AV, Arzhanov MM, Demchenko PF, Denisov SN, Karpenko AA (2008c), Modelling of changes in high latitudes using the IAP RAS climate model. In: Kotlyakov VM (ed) Changes of natural environment and climate: natural and possible consequent human-induced catastrophes, v II, environmental processes in the polar regions of the earth. IG RAS, Moscow (in Russian)

Myhre G, Highwood EJ, Shine KP, Stordal F (1998) New estimates of radiative forcing due to well mixed greenhouse gases. Geophys Res Lett 25:2715–2718

Rasch PJ, Crutzen PJ, Coleman DB (2008a) Exploring the geoengineering of climate using stratospheric sulfate aerosols: the role of particle size. Geophys Res Lett 35:L02809. doi:10.1029/2007GL032179

Rasch PJ, Tilmes S, Turco RP, Robock A, Oman L, Chen C-C, Stenchikov GL, Garcia RR (2008b) An overview of geoengineering of climate using stratospheric sulphate aerosols. Philos Trans R Soc, Ser A 366:4007–4037

Robock A (2000) Volcanic eruptions and climate. Rev Geophys 38:191–219

Robock A, Oman L, Stenchikov GL (2008) Regional climate responses to geoengineering with tropical and arctic SO_2 injections. J Geophys Res 113:D16101. doi:10.1029/2008JD010050

Schneider SH (1996) Geoengineering: could—or should—we do it? Clim Change 33:291–302

Schneider SH (2001) Earth systems engineering and management. Nature 409:417–421

Shvidenko A, Nilsson S (2003) A synthesis of the impact of Russian forests on the global carbon budget for 1961–1998. Tellus 55B:391–415

Smith SJ, Pitcher H, Wigley TML (2001) Global and regional anthropogenic sulfur dioxide emissions. Glob Planet Change 29:99–119

Solomon S (1999) Stratospheric ozone depletion: a review of concepts and history. Rev Geophys 37:275–316

Stern DI, Kaufmann RK (1996) Estimates of global anthropogenic methane emissions 1860–1993. Chemosphere 33:159–176

Stocker TF, Schmittner A (1997) Influence of CO_2 emission rates on the stability of thermohaline circulation. Nature 388:862–865

Stowe LL, Carey RM, Pellegrino PP (1992) Monitoring the Mt. Pinatubo aerosol layer with NOAA/11 AVHRR data. Geophys Res Lett 19:159–162

Tilmes S, Muller R, Salawitch R (2008) The sensitivity of polar ozone depletion to proposed geoengineering schemes. Science 320:1201–1204

Trenberth KE, Dai A (2007) Effects of Mount Pinatubo volcanic eruption on the hydrological cycle as an analog of geoengineering. Geophys Res Lett 34:L15702. doi:10.1029/2007GL030524

Trenberth KE, Jones PD, Ambenje P, Bojariu R, Easterling D, Klein Tank A, Parker D, Rahimzadeh F, Renwick JA, Rusticucci M, Soden B, Zhai P (2007) Observations: surface and atmospheric climate change. In: Solomon S, Qin D, Manning M, Marquis M, Averyt K, Tignor MMB, LeRoy Miller H, Chen Z (eds) Climate Change 2007: the physical science basis. Cambridge University Press, Cambridge, pp 235–336

Wigley TML (2000) ENSO, volcanoes and record-breaking temperatures. Geophys Res Lett 27:4101–4104

Wigley TML (2006) A combined mitigation/geoengineering approach to climate stabilization. Science 314:452–454

Zerefos CS, Tourpali K, Bais AF (1994) Further studies on possible volcanic signal to the ozone layer. J Geophys Res 99:25741–25746